Adsorption of Organic Dyes onto Commercial Activated Carbon by Using Non-linear Regression Method

Hadjer Zeghache[1*], Said Hafsi[1], and Noureddine Gherraf[2]

[1]Laboratory of Applied Chemistry and Material Technology,
Materials Sciences Department, Larbi Ben M'Hidi, university, Algeria
[2]Laboratory of Natural Resources and Management of Sensitive Environments,
Larbi ben M'Hidi university, Algeria

* Corresponding author: hadjerzeghache@yahoo.com
Received: June 5, 2018; Accepted: August 30, 2018

Abstract

The present paper intends to appraise the influencing operative variable on the adsorption efficiency of two organic dyes namely Erythrosine and Brilliant green on activated carbon in aqueous solution. The experimental data at equilibrium were studied through the non-linear regression of Langmuir, Freundlich and Liu isotherm models. Collected data and obtained results seems to fit well with the Liu model for both dyes with R^2_{adj} values closer to one and lower values of SD. The kinetic behaviors of solute adsorption were respectively employed by using different existing models, Pseudo-first, Pseudo-second order, General order, Avrami and Elovich equation. Findings results showed that General order had more conformity compared with the others, for Brilliant green with $R^2 adj =0.9949$ and Avrami kinetic model for Erythrosine with $R^2_{adj} = 0.9956$. According to the calculated thermodynamic parameters the adsorption process of the Erythrosine dye is endothermic and spontaneous process in nature ($\Delta H^0=41.428-41.459 KJ/mol$) and non-spontaneous for the Brilliant green dye ($\Delta H^0=80.409-54.955 KJ/mol$) over the studied temperatures (293K-303K).

Keywords: Erythrosine; Brilliant green; Activated carbon; Isotherm; kinetic; Non-linear regression.

1. Introduction

Discharging of noxious residues from dyeing industries into environment leads to a serious risk to living aquatic organisms and human health. The existence of an extremely small concentration of dyes in water can be perilous because most of them are poisonous and carcinogenic. Furthermore, some of them have complicated aromatic structures, which render them more stable and difficult to remove (Ghaedi *et al.*, 2018; Karimifard and Moghaddam., 2018; Zazouli *et al.*, 2016; Rahman *et al.*, 2018). Consequently, their discoloration and reduce from industrial effluents before discharge into a range of receiving environments is exceedingly vital and continues to be problematic (Uday *et al.*, 2017; Uruj *et al.*,2016; Heibati *et al.*, 2015). Erythrosine and brilliant green are some of the prevalent synthetic dyes, which are used in the

cloth industry, pharmaceutical, cosmetic, and food. These dyes are regarded as an irritant of the skin, eye burns, and gastrointestinal symptoms with nausea, vomiting, diarrhea. It may also cause learning difficulties (hyperactivity) and sensitivity to light (Al-Degs *et al.*, 2012; Karimi *et al.*, 2016; Salem *et al.*, 2015; Kumar *et al.*, 2014; Roosta *et al.*, 2014). There are many dyes removal techniques as ion exchange, electro-coagulation, coagulation-flocculation, oxidation, reverse osmosis, adsorption, photocatalytic degradation, and nano-filtration. Nevertheless, adsorption on activated carbon is regarded as an efficient and popular approach largely adopted for industrial treatment. The main advantage of this method is removing a wide range of toxic effluents in a single run, which lead to high quality of treated wastewaters in a short time with flexibility in design and operation (Abid *et al.*, 2012; Li *et al.*, 2017; Doczekalska *et al.*, 2018; Mukhlish *et al.*, 2016; Castañeda - Díaz *et al.*, 2017; Deng *et al.*, 2015; Carneiro *et al.*, 2016; Wawrzkiewicz *et al.*, 2015; Buscio *et al.*, 2016). Activated carbon is one of the best and effective adsorbents used for many applications due to a higher degree of porosity and extended surface area, leading to a high adsorbent capacity (Corda and Srinivas, 2018; Di Biase and Sarkisov, 2015; Anisuzzaman *et al.*, 2015). In order to estimate the efficiency in the removal of erythrosine and brilliant green onto granular activated carbon, statical optimization of the influential variables (initial concentration, agitation speed, pH and temperature), was well evaluated and elucidated using batch method experiments. Modeling of kinetic adsorption and isotherm parameters were also assessed to understand the mechanism of adsorption between the adsorbates and adsorbent.

2. Materials and methods

2.1 Adsorbent

The specific surface area of granular activated carbon (CAG) of vegetable origin which is produced by Prolabo with a particle size < 3 mm, carried out in a Micromeritics ASAP 2020 with nitrogen at 77K exhibits a hysteresis for which the desorption branch joins the adsorption branch for a relative pressure equal

to 0.42 (Figure 1). This hysteresis is significant in the presence of mesoporous (type IV isotherm) (Thommes *et al.*, 2015; Jayaraman, 2017). The CAG had specific area equal to ~ 988 m^2 /g determined by plotting the curve $\frac{P_r}{V_{ads}(1-P_r)}$ versus Pr (Pression). with the pore diameter of 36 A° (pore diameter greater than 20 A°), thus, it has a mesoporous texture.

2.2 Selected dyes

Two organic dyes produced from Merck were chosen as model adsorbates. Brilliant green is one of common basic dyes in the class of triarylmethane dye (sulfate of di-(p-diethylamino) triphenyl carbonyl anhydride) and Erythrosine which is an organ-iodine compound derived from fluorine presented under the form of disodium salt of 2, 4,5,7 tetraiodfluorescein were chosen because of their different structures (Table 1 and Figure 2).

The determination of the concentration of the molecules adsorbates in aqueous solution was measured through a molecular absorption spectro-photometry (Spectronic70 Spectro-photometer). It has been calculated by referring to the calibration curve obtained by linear fitting from test solutions at a wavelength (λ_{max}) corresponding to the maximum absorbance for each dye (Table 1 and Figure 3). Eq. 1 was used to calculate the adsorption quantity of dyes adsorbed on granular activated carbon at the time t (Manera *et al.*, 2018).

$$q_t = \frac{Co - Ct}{m} \times v \qquad \text{Eq. 1}$$

The amount adsorbed at Eq. 1, qe, was calculated using Eq. 2 (Gautam *et al.*, 2015).

$$q_e = \frac{Co - Ce}{m} \times v \qquad \text{Eq. 2}$$

Where, q_t: quantity of adsorbate adsorbed at time t (mg/g), C_0 and C_t:initial and remaining concentration (mg/l) of dye in solution respectively ,q_e: dye adsorbed quantity (mg/g) per unit mass of activated carbon at equilibrium, C_e: remaining concentration (mg/L) of dye at equilibrium V: the volume (L) of dye solution and m is the weight (g) of the activated carbon.

**Table 1.** Main characteristics of dyes used with different forms.

Dye	Brilliant green	Erythrosine
C.I.name	C.I. 42040	C.I. 45430
Molecular Formula	$C_{27}H_{34}N_2O_4S$	$C_{20}H_6I_4Na_2O_5H_2O$
Molecular weight (g/mol)	482.64	897.88
λ_{max}(nm)	623 nm	527 nm
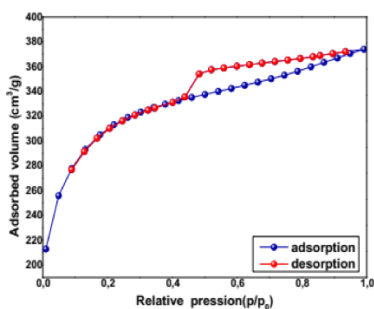
Figure1. Isotherm adsorption-desorption of nitrogen on commercial activated carbon.
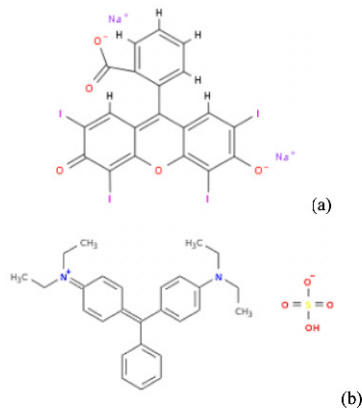
Figure 2. Chemical structure of Erythrosine (a) and Brilliant green (b).
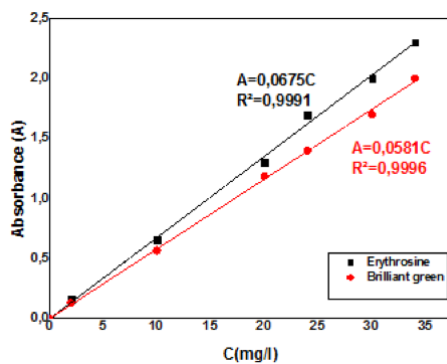
Figure 3. Calibration curves for Erythrosine and Brilliant green solutions.

3. Results and discussion

3.1 SEM micrographs

The external surface topography of CAG is identified by SEM scanning electron microscope (Joel-JSM-6360L V) scanning electron microscope, and the results are showed in figure 4. As shown the surface of CAG had considerable numbers of pores where dyes can be caught and adsorbed. The microscope analysis of CAG sample before adsorption shows specific dark spots, revealing a big eventuality, for adsorbing dye molecules in the pores. Apparent reduction of dark spots can be noticed in Figure 4 (B and C) deduced as a sign of presence of dyes on the surface of CAG.

3.2 Effect of initial concentration on adsorption ability

The effect of the initial concentration on adsorption ability of both dyes was inspected with varying the concentration between 15 and 45 mg /l. The analysis curves are shown in Figure 5 demonstrates that the raise of initial of initial concentration leads to an increase of adsorbed dyes. As an indication, the amount of adsorbed dyes increased from 0.373 to 1.10 mg/g in case of erythrosine and from 0.371 to 1.09 mg/g in case of brilliant green during a contact time of 210 min, this might be due to an increase in the number of collisions between the adsorbates and the adsorbent, hence enhancing the adsorption rate. Similar conclusions on the effect of adsorbate concentration on the removal behavior have been proposed by (Albroomi *et al.*, 2016) for the adsorption of tartrazine by activated carbon prepared from apricot stones.

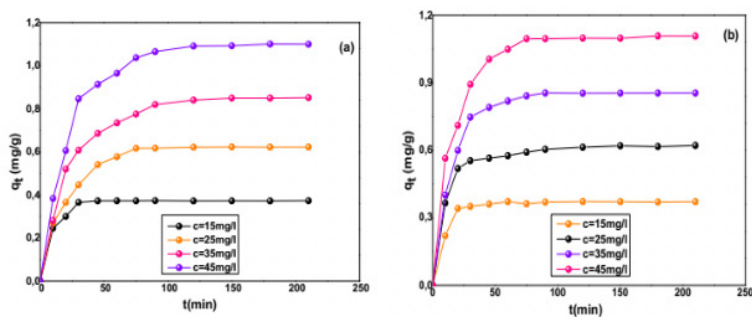## 3.3 Effect of agitation speed on adsorption ability

The agitation speed is essential parameter to ensure the transfer of solute molecules to the adsorbent. The curves in Figure 6 illustrate the consequence of agitation speed on dyes elimination of erythrosine and brilliant green in the range of 60 to 275 rpm. It is apparent in the figure that the increase of agitation speed leads to an increase of adsorbed dyes. As an indication, the quantity of erythrosine adsorbed increased from 0.76 to 0.86 mg/g and that of brilliant green from 0.77 to 0.87 mg/g when the agitation speed varies from 60 to 275 rpm during a contact time of 210 min. Because of the fact that the raise in the agitation speed provides good homogenization of the solution in order to achieve the equilibrium state and leads to a decrease in diffusion layer thickness surrounding the adsorbent surface (Prashanthi *et al.*, 2017). The increase of the adsorption rate with the agitation speed was also reached for the adsorption of 4-chlorophenol on granular activated carbon (Kusmierek and Swiatkowski, 2015) as well as the adsorption of red violet on montmorillonite clay (Fil *et al.*, 2014).
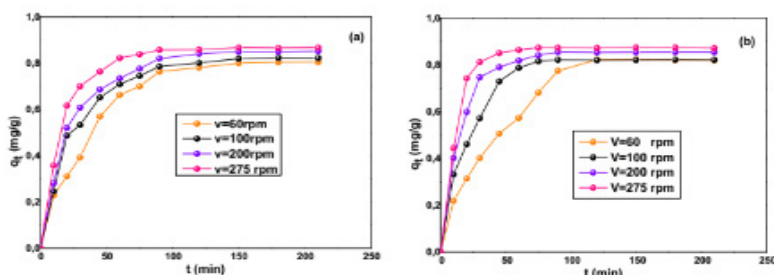
3.4 Effect of initial pH on adsorption ability

As well-known, the pH is one of an operative parameter influenced in practically the adsorption capacity because it plays a primary role to the adjustment of the adsorption facility of adsorbent, controls the charge in surface of the adsorbent and affects the ionization level of the dye in the solution. To evaluate the pH effectiveness on dyes removal by CAG, a series of experiments at different pH between 3 and 11 was conducted. From Figure 7, it was observed that the pH has an obvious influence in the extent of adsorption.

The adsorption capacity of brilliant green (Figure 7-b) was found favorably increased at increasing values of pH which is associated with the negative charge on CAG surface and the positive charge of brilliant green (cationic dye). At acidic pH values, the number of positively charged sites on the adsorbent surface increased which enhance the positively charged of brilliant green through an electrostatic force of repulsion which caused a diminished in the removal efficiency. A similar behavior was studied on the removal of cationic dye on sepiolite and malachite green on modified (MIL-101-SO$_3$H) (Demirbas *et al.*, 2014; Luo *et al.*, 2017) .Contrarily when the pH of erythrosine dye solution becomes low (pH≤4) the adsorption capacities increased (Figure 7-a). The presence of H$^+$ ions as functional group at low pH increases the number of positive charges of adsorbent in spite of the negative charge of the dye (anionic dye), indicating an electrostatic attraction between the adsorbate and adsorbent with a highest
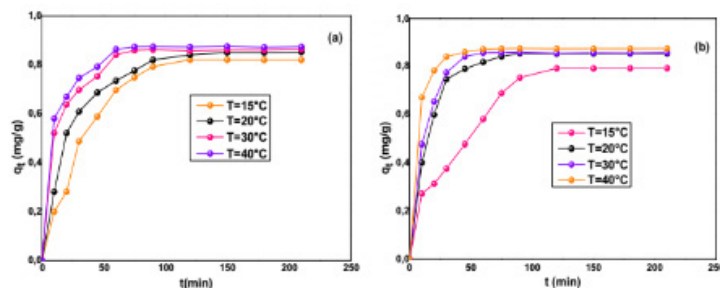
Figure 5. Effect of initial concentration on adsorption ability of Erythrosine (a) and Brilliant green (b). Experimental conditions: m=1000 mg, v=200 rpm, T=293K, pH=9,03 ,5,2 and V=25ml.

Figure 6. Effect of agitation speed on adsorption ability of Erythrosine (a) and Brilliant green (b). Experimental conditions: m=1000 mg, C0=35 mg/L, T=293K, pH=9,03 ,5,2 and V=25ml.
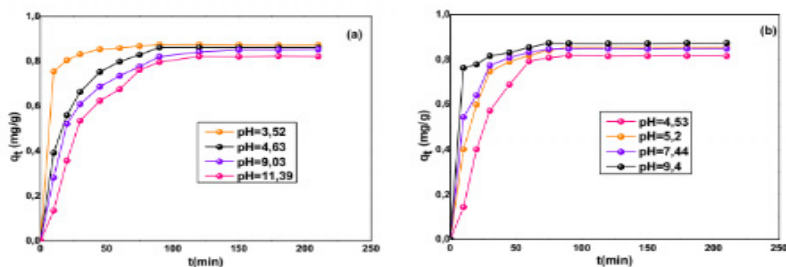
Figure 7. Effect of pH values on adsorption ability of Erythrosine (a) and Brilliant green (b). Experimental conditions: m=1000 mg, C0=35 mg/L, v=200 rpm, T=293K and V=25ml.

Figure 8. Effect of solution temperature on adsorption ability of Erythrosine (a) and Brilliant green (b). Experimental conditions: m=1000 mg, C0=35 mg/L, v=200 rpm, pH=9,03 ,5,2 and V=25ml.

value of adsorbed quantity at pH 3.52 for 60 min contact time. At higher pH (pH≥9), the presence of OH- on the surface of adsorbent might not support the sorption of anionic dye. The similar trends were seen for removal of RB5 on DMAC16, acid red 57 on calcined-alunite and brilliant blue R using Amino-Functionalized Organosilane (Erdem *et al.*, 2016 ;Tunali *et al.*, 2016; Saputra *et al.*, 2017).

3.5. Effect of solution temperature on adsorption ability

The temperature was an influencing parameter to understand the bonding between the adsorbent surface and substance adsorbed; it was evaluated within the range 288K to 313K. According to the curves of Figure 8, the equilibrium time increases as temperature increases shifting from 120 min for T=288K to 50 min for 313K.This may be justified by increasing the particles motion and hence promoting their incursion into the pores of the activated carbon. Additionally, the solution viscosity reduces by rising the temperature leading to an increase in the rate of diffusion of the adsorbates across the outside boundary layer, which in turn, enhances the adsorption ability (El Haddad *et al.*, 2013).

4. Determination of adsorption isotherm parameters

A nonlinear form of adsorption isotherms were simulated by using several models, such as: Langmuir, Freundlich and Liu for describing the partition of dyes between solid phase and the solution, in order to discuss the experimental characteristics of the adsorption isotherms.

4.1 Langmuir isotherm
The model is depended on the following assumptions: (Gurdeep ,2000; Li *et al.*, 2012) homogeneous sites within the adsorbent (all binding sites having the same energy), Absence of Interactions between the adsorbed molecules, All adsorption take place through the same mechanism, Formation of an adsorbate monolayer coverage the surface of the adsorbent, Each site can react only with one adsorbate species.

The Langmuir equation gives as Eq. 3.

$$q_e = \frac{q_m K_L C_e}{1 + K_L C_e} \qquad \text{Eq.3}$$

Where, q_e is the quantity of adsorbed dye per unit activated carbon mass (mg/g),q_m: utmost adsorption capacity (mg/g), K_L: equilibrium constant related to affinity of binding sites (L/mg) ,C_e: residual concentration of dye at equilibrium (mg/L).

4.2 Freundlich isotherm
Freundlich gaves an experiential expression used to explicate the adsorption properties over different surfaces. It is often conveyed by the Eq. 4 (Freundlich, 1906):

$$q_e = K_F C_e^{1/n} \qquad \text{Eq.4}$$

Where, K_F: Partition coefficient constant of Freundlich in equilibrium (mg $^{(1-n)}$L^n/g), n_F : Intensity and capacity of adsorption (Without units).

4.3 Liu isotherm
The Liu model can be regarded as an arrangement of both Langmuir and Freundlich isotherms without assumption, in general is based on the fact that the binding sites are energetically different. Consequently, the adsorbent active sites may exhibit different affinities towards adsorbate molecules; however, saturation of the active sites should occur in a different manner of that of the Freundlich model. Eq. 5 expressed the mathematical relation of Liu isotherm model (Liu *et al.*, 2003; Bergmann *et al* .,2015; Dos Santos *et al* ., 2015):

$$q_e = \frac{q_{max}(K_g C_e)^{n_L}}{1 + (K_g C_e)^{n_L}} \qquad \text{Eq.5}$$

Where K_g: equilibrium constant of Liu isotherm (L/mg), n_L: exponent of the Liu equation (dimensionless).

5. Error functions

In recent decades the parameters of the preceding isotherms estimated by linear regression, which is widely used as one of the most common method for best fitting. Most

of works was based on the choice of a mathematical model on the value of R² (correlation coefficient). However, the use of only one R² may not be sufficient for comparing the goodness of fit. This is because of the distribution of error changes either the worst or the best and fit distortion (Foo *et al.*, 2010). For this, we use the nonlinear regression in this study to minimize errors that may be introduced between the predicted data and experimental color removal by subjecting on the convergence criteria as an adequate method (Belhachemi and Adoun,2011). With a comparison of two previous methods, statistically, the more appropriate and estimate method obtained by nonlinear regression model (Srenscek-Nazzal *et al.*, 2015; Özdemir and Önal, 2013; Boulinguiez *et al.*, 2008, Largitte and Pasquier, 2016). Different type of error functions have been used for testing the result of a regression model for residue analysis. In this context, we chose five types of statistical functions among the most widely used in such studies, which are represented by Eqs.6 to 10, respectively (Machado *et al.*, 2011).

5.1 Residual sum of squares (RSS)

$$RSS = \sum_{i=1}^{n}(q_{i,observed} - q_{i,calc})^2 \quad \text{Eq. 6}$$

5.2 Reduced Chi-squared (X^2_{red})

$$X^2_{red} = \sum_{i=1}^{m}\frac{(q_{i,observed} - q_{i,calc})^2}{N - P} \quad \text{Eq.7}$$

5.3 Standard deviation (SD)

$$SD = \sqrt{(\frac{1}{N-P})\sum_{i=1}^{n}(q_{i,observed} - q_{i,calc})^2} \quad \text{Eq.8}$$

5.4 Coefficient of determination (R²)

$$R^2 = \left[\frac{\sum_{i=1}^{n}(q_{i,observed} - \bar{q}_{observed})^2 - \sum_{i=1}^{n}(q_{i,observed} - q_{i,calc})^2}{\sum_{i=1}^{n}(q_{i,observed} - \bar{q}_{observed})^2}\right] \quad \text{Eq.9}$$

5.5 Adjusted R-squared

$$R^2_{adj} = 1 - (1 - R^2)\left(\frac{N-1}{N-P-1}\right) \quad \text{Eq.10}$$

Where, N: total number of experimental data and P: the number of parameters of the fitted model, R²: coefficient of determination.

The most suitable model should have a minimum value of SD and R^2_{adj} equals almost one (Bergmann and Machado, 2015). The results of modeling data for both dyes onto activated carbon are summarized up in Tables 2. We note that the Langmuir constant K_L increases with increasing temperature for both dyes. As the value of K_L measures the intensity of adsorption, we deduce that affinity between the adsorbates and activated carbon increases as the temperature elevated from 293K to 303 K. Comparing the Adjusted R- squared values (R²adj) between the erythrosine and brilliant green dye, the results showed that the Langmuir model is favorably adapted for adsorbed erythrosine than brilliant green dye at different ranges of temperature.

The Freundlich exponent n is bigger than 1, indicating a favorable adsorption of erythrosine and brilliant green at experimental conditions (El-Sayed *et al.*, 2014). The error calculations show that the Liu isotherm model turns out to be suitable for both dyes compared with the two other models (Liu>Langmuir>Freundlich). The Liu model is well adapted to describe the adsorption of erythrosine and brilliant green on activated carbon.

The peak adsorption capacity of brilliant green and erythrosine dyes by other potential adsorbents are given in Table 3. As depicted, the qmax of brilliant green onto granular activated carbon was higher value than the other values and for erythrosine dye, it was average value compared to the adsorbents listed. However, the entire of modeling results proved that the CAG fits very well as promising adsorbent on cationic and anionic dyes removal.

6. Adsorption kinetics modelling

A number of adsorption kinetic was evaluated to optimize the adsorption mechanism pathways, with examining the rate of adsorption procedure, several models in this study was undertaken to investigate the kinetic data.

6.1 Pseudo-first-order kinetic model

The Lagergren model was discovered initially as non–reversible equation (Lagergren.,

Table 2. Non-linear regression parameters of adsorption isotherm models of Erythrosine and Brilliant green on activated carbon with error analysis.

	Erythrosine			Brilliant green		
T(K)	293	298	303	293	298	303
			Langmuir			
K_L	1.0847	1.2077	1.9052	0.1404	0.2032	0.4182
q_m	4.2869	4.7727	4.4357	5.5442	5.4057	4.5535
RSS	0.0228	0.0639	0.1040	0.2028	0.0589	0.1741
$X^{2\,red}$	0.0045	0.01279	0.0208	0.0405	0.0117	0.0348
SD	0.0675	0.1130	0.1442	0.2014	0.1085	0.1866
R^2	0.9975	0.9932	0.9890	0.9757	0.9931	0.9802
R^2_{adj}	0.9970	0.9918	0.9868	0.9708	0.9918	0.9762
			Freundlich			
K_F	2.2520	2.5814	2.8242	1.0651	1.2412	1.7380
n	3.0257	2.7154	3.2393	2.0822	2.0905	2.9360
RSS	0.0898	0.1968	0.2743	0.3053	0.1295	0.3373
$X^{2\,red}$	0.0179	0.0393	0.0548	0.0610	0.0259	0.0674
SD	0.1340	0.1982	0.2340	0.2471	0.1609	0.2597
R^2	0.9902	0.9790	0.9709	0.9634	0.9849	0.9616
R^2_{adj}	0.9882	0.9749	0.9651	0.9561	0.9819	0.9540
			Liu			
K_g	1.2538	1.5988	2.1998	0.2391	0.3321	0.5037
q_{max}	3.9025	3.8059	3.6434	3.4672	3.9698	3.4808
n_L	1.2657	1.8192	2.0645	3.1313	1.6790	2.6407
RSS	0.017	0.0020	0.0043	0.01361	0.0266	0.0055
X^{2red}	0.0042	5.01×10^{-4}	0.0010	0.0034	0.0066	0.0013
SD	0.0651	0.0223	0.0328	0.0583	0.0815	0.0372
R^2	0.9981	0.9997	0.9995	0.9983	0.9969	0.9993
R^2_{adj}	0.9972	0.9996	0.9993	0.9975	0.9953	0.999

1898), and validated in general, in the first minutes of the adsorption phenomena (Eq.11)

$$\frac{dq_t}{dt} = K_1(q_e - q_t) \qquad \text{Eq.11}$$

Where, k1: rate constant ofpseudo-first-order sorption (min⁻¹). Equation (12) can be presented by:

$$q_t = q_e(1 - \exp(k_1 t)) \qquad \text{Eq.12}$$

6.2. Pseudo-second-order kinetic model

This model is described by Ho and Mckay it is valid for a wide range of time and requires a chemisorption mechanism (Ho and Mckay ,1999). It expression as:

$$\frac{dq_t}{dt} = k_2(q_e - q_t)^2 \qquad \text{Eq.13}$$

The integration of Eq. (13) leads to the non-linear form:

$$q_t = \frac{k_2 q_e^2 t}{1 + k_2 q_e t} \qquad \text{Eq.14}$$

The advantage of using the non-linear form lies directly on the fact that we do not need to know the equilibrium capacity q_e from experience, since it can be determined from the model. This makes it possible to determine K_2 and the initial rate of adsorption Eq. (15).

$$h_0 = K_2(q_e)^2 \qquad \text{Eq.15}$$

Where, K_2: pseudo-second-order model rate constant ($g.mg^{-1}.min^{-1}$), h_0: initial sorption rate for pseudo-second-order adsorption (mg/g/min).

6.3 Avrami fractionary kinetic model

The exponential function of Avrami model was made to check specific changes of kinetic thermal parameters, original concentration, and adsorption time. Avrami model is expressed mathematically by Eq.16 (Bergmann and Machado, 2015; Inyinbor *et al.*, 2016; Mohd *et al.*, 2014).

$$q_t = q_e(1 - \exp(-K_{av} - t)^{nAV} \quad \text{Eq.16}$$

Where, k_{AV}: Adjusted kinetic constant (min^{-1}), n_{AV}: fractional adsorption order.

6.4 General order kinetic model

The model relies on the number of accessible sites on the surface of adsorbent. It is given in Eq. 17 (Bergmann and Machado, 2015):

$$q_t = q_e - \frac{q_e}{\left[K_N(q_e)^{n-1}.t.(n-1)+1\right]^{1/1-n}} \quad \text{Eq.17}$$

with $n \neq 1$, Where: k_N: kinetic adsorption rate constant ($min^{-1}.(g/mg)n^{-1}$), n: order of adsorption.

6.5 Elovich model

Another rate equation called as Elovich model, in general applied successfully in chemical adsorption kinetics (Mclintock, 1967). It assumes that the adsorption sites increase exponentially with adsorption followed by a slow rate diffusion. Which implies heterogeneous adsorbing surface (Zhang *et al.*,2017).It given in the mathematical Eq. 18.

$$\frac{dqt}{dt} = \alpha \exp(-\beta q_t) \qquad \text{Eq.18}$$

The integration of equation 18 give as Eq. 19.

$$q_t = \frac{1}{\beta}\ln(\alpha\beta) + \frac{1}{\beta}\ln(t) \qquad \text{Eq.19}$$

Where, α: initial adsorption rate (mg/g/min^{-1}), β: adsorption constant related to the surface coverage (g/mg).

It is essential to studied precisely the kinetics adsorption to find best fit of two organic dyes on CAG, five kinetics models were tested by using nonlinear method as shown in figure 9. The determination of experimental kinetic adsorption parameters was recapitulated in Table 4. As referred in Table 4, the calculated adjacent R squared are closer to unity and the error functions values (SD,) are smaller for avrami kinetic model than general kinetic order and pseudo-first order. Therefore with comparing the results of the five kinetics models the best

Table 3. Maximum dye removal capacity for Brilliant green and Erythrosine by some potential adsorbents.

Dye	Adsorbent	Maximum dye removal capacity (mg/g)	References
Brilliant green	Activated carbon prepared from acorn	2.1	(Ghaedi *et al.*,2011)
	Psidium guajava (Guava) leaves	1.075	(Rehman *et al.*,2015)
	peels of Solanum tuberosum (Potato)	1.173	(Rehman *et al.*,2015)
	Granular activated carbon (CAG)	5.405	Current study
Erythrosine	Pumpkin seed hulls	5.03	(Apostol *et al* .,2015)
	De-oiled mustard active carbon	3.46	(Jain *et al.*,2009)
	Cellulose granules	3,75	(Tabara *et al.*,2011)
	Granular activated carbon (CAG)	4.77	Current study

fit were obtained for Avrami kinetic model for erythrosine dye with R^2_{adj} equal to 0.9959. This is compatible with previous literature work like the sorption of Procion Red MX 3B onto brazilian pine fruit shell (Calvete *et al.*, 2009). Moving to the case of brilliant green, the modeling of adsorption kinetics is in accordance with the general order model (R^2_{adj}=0.9949) at T=293K and it may also, support the second order kinetic and avrami model. Similar studies was reported on the adsorption process of tetracycline antibiotic on Zn-AC and methylene blue on canola residues (Takdastan *et al.*, 2016; Balarak *et al.*, 2015), therefore the adsorption capacity at equilibrium is very close to experimental values by the appropriate model for each dye.

7. Thermodynamic study

The constants of the Langmuir and Liu isotherms (K= Kg or KL) depend on temperature, consequently they can be used for estimating the thermodynamic quantities on adsorbed dyes by CAG, such as standard free energy change (ΔG°), isosteric adsorption enthalpy (ΔH°) and isosteric adsorption entropy(ΔS°) it was calculated as follows (Gopinathan *et al.*, 2016):

$$\Delta G^o = -RT \ln K \qquad \text{Eq.20}$$

$$\Delta G^o = \Delta H^o - T\Delta S^o \qquad \text{Eq.21}$$

$$\ln K = \frac{\Delta S^o}{R} - \frac{\Delta H^o}{RT} \qquad \text{Eq.22}$$

Where, K is the binding constant, R is universal gas constant (8,314J/mol/K) and T is the experimental temperature (K). When the lnK is plotted versus the inverse of the temperature gives a straight line with the slope -ΔH°/R , and intercept ΔS°/R . The calculations results are given in Table 5. The Liu model showed the highest values of for both of dyes, which means that the values calculated of standard entropy and enthalpy, were reliable. In addition the positive and low ΔH° values shows that their interaction was an endothermic process of erythrosine and brilliant green adsorption on activated carbon. The negative ΔG° values indicated that the binding of erythrosine with activated carbon is a spontaneous physiosorption process (ΔG°<-20K J/mol) (Balarak *et al* ., 2016), and the spontaneity increases with temperature. On the other hand, in the case of brilliant green the values of ΔG° is positive accompanied by decrease with increasing the temperature. Thus indicating an increase in thermodynamic feasibility at higher temperatures (Regti *et al.*, 2017), The calculations results are given in Table 5. The Liu model showed the highest values of for both of dyes, which means that the values calculated of standard entropy and enthalpy, were reliable. In addition the positive and low ΔH° values shows that their interaction was an endothermic process of erythrosine and brilliant green adsorption on activated carbon. The negative ΔG° values indicated that the binding
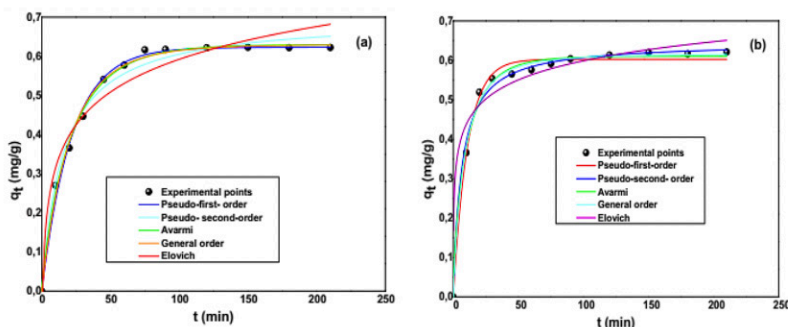

Figure 9. The curves of the five nonlinear modelled kinetics adsorption of Erythrosine (a) and Brilliant green (b) on activated carbon at T=293K.

Table 4. Experimental results of kinetic modeling of brilliant green and erythrosine on activated carbon.

Kinetic models and its parameters	Erythrosine	Brilliant green
qe(exp)	0.6218	0.61338
Pseudo-first order		
k_1	0.0462	0.0922
q_e(cal)	0.623	0.6026
RSS	0.0023	0.0027
$X^{2\ red}$	2.35×10^{-4}	2.72×10^{-4}
SD	0.0153	0.0173
R^2	0.9943	0.9922
R^2_{adj}	0.9938	0.9914
Pseudo-second order		
k_2	0.0924	0.2445
q_e(cal)	0.6991	0.6454
h0	0.0451	0.1018
RSS	0.00519	0.0023
$X^{2\ red}$	5.18×10^{-4}	2.99×10^{-4}
SD	0.0227	0.0173
R^2	0.9875	0.9934
R^2_{adj}	0.9863	0.9927
Elovich		
α	0.1634	3.688
β	8.2859	14.3108
RSS	0.0177	0.00102
$X^{2\ red}$	0.0017	0.00103
SD	0.0421	0.032
R^2	0.9574	0.9707
R^2_{adj}	0.9532	0.9678
General order		
qe(cal)	0.6298	0.6173
kN	0.0533	0.1482
n	1.1469	1.4488
RSS	0.001	0.0014
X^2	2.26×10^{-4}	1.62×10^{-4}
SD	0.015	0.0127
R^2	0.9951	0.9958
R^2_{adj}	0.994	0.9949
Avrami		
q_e(cal)	0.6298	0.6103
$_kAV$	0.046	0.0969
$_nAV$	0.8764	0.7561
RSS	0.0014	0.002
$X^{2\ red}$	1.65×10^{-4}	2.31×10^{-4}
SD	0.0127	0.0152
R^2	0.9964	0.994
R^2_{adj}	0.9956	0.9927

Table 5. Thermodynamic parameters of dyes adsorption onto activated carbon.

	Erythrosine						Brilliant green					
T(K)	293	298	303	293	298	303	293	298	303	293	298	303
Isotherm	Langmuir			Liu			Langmuir			Liu		
ΔS^0 (J/K/mol)	141 .581			143 .263			257.607			175.526		
ΔH^0 (KJ/mol)	41.428			41.459			80.409			54.955		
ΔG^0 (KJ/mol)	-0.19	-0.47	-1.62	-0.55	-1.16	-1.98	4.78	3.94	2.19	3.49	2.73	1.72

of erythrosine with activated carbon is a spontaneous physiosorption process ($\Delta G° < -20K$ J/mol) (Balarak *et al* ., 2016), and the spontaneity increases with temperature. On the other hand, in the case of brilliant green the values of $\Delta G°$ is positive accompanied by decrease with increasing the temperature. Thus indicating an increase in thermodynamic feasibility at higher temperatures (Regti *et al.*, 2017).

8. Conclusions

This study dealt with the application of activated carbon as an effective sorbent for rapid removal of two organic dyes in aqueous solution. Different parameters related to the operating conditions (initial concentration of dye, pH, stirring speed, and temperature) were estimated by batch tests. For all kinetic data the adsorption mechanism provided the best correlation by a kinetic of the Avrami model in case of erythrosine with R^2_{adj} =0.9956 and general order in case of brilliant green with R^2_{adj}= 0.9949. The plot of experimental adsorption isotherm data for both dyes favorably followed the Liu isotherm model. The obtained results of thermodynamic effect proved that the adsorption of the erythrosine dye is endothermic and spontaneous process in nature and non- spontaneous for the brilliant green dye within the limits of physical adsorption.

Acknowledgement

References

Abid MF, Zablouk MA. Muhssen A, Alameeet A. Experimental study of dye removal from industrial wastewater by membrane technologies of reverse osmosis and nanofiltration. Iranian Journal of Environnemental Hea1th Science& Enginnering 2012; 9 :7.

Albroomi HI, Elsayed MA , Baraka A, Abdelmaged MA. Batch and fixed-bed adsorption of tartrazine azo-dye onto activated carbon prepared from apricot stones . Applied Water Science 2016; 7:2063–2074.

Al-Degs YS, Abu-El-Halawa R, Abu-Alrub SS. Analyzing adsorption data of erythrosine dye using principal component analysis. Chemical Engineering 2012 ;191 : 185–194.

Amin T, Alazba A A, Shafiq M. Adsorptive Removal of Reactive Black 5 from Wastewater Using Bentonite Clay: Isotherms, Kinetics and Thermodynamics . Sustainability 2015;7

Anisuzzaman SM, Joseph CG,Taufiq-Yap YH, Duduku Krishnaiah , Tay VV. Modification of commercial activated carbon for the removal of 2,4-dichlorophenol from simulated wastewater. Journal of King Saud University – Science 2015; 27: 318–330.

Apostol LC, Ghinea C, Alves M, Gavrilescu M. Removal of Erythrosine B dye from water effluents using crop waste pumpkin seed hulls as adsorbent. Desalination Water and Treatment 2015;1–24.

Balarak D, Jaafari J, Hssani G, Mahdavi Y, Tyagi I, Agarwal S, Gupta V K .The use of low-cost adsorbent (Canola residues) for the adsorption of methylene blue from aqueous solution: Isotherm, kinetic and thermodynamic studies

.Colloids and Interface Science Communications 2015 ;7:16-19.

Balarak D, Mahdavi Y,Bazrafshan E,Mahvi A H. .Kinetic, isotherms and thermodynamic modelling for adsorption of acid blue 92(AB92) from aqueous solution by modified azolla filicoloides. Fresenius Environmental bulletin 2016 ;5:1322-1331.

Belhachemi M, Addoun F. Comparative Adsorption. Isotherms and Modeling of Methylene Blue onto Activated. Carbons. Applied Water Science 2011 ;1:1 11–117.

Bergmann CP,Machado MF.Carbon Nanomaterials as Adsorbents for Environmental and Biological Applications. Carbon Nanostructures .Springer ; 2015.

Boulinguiez B, Le Cloirec,P, Wolbert D.Revisiting the determination of langmuir parameters—application to tetrahydrothiophene adsorption onto activated carbon .Langmuir 2008; 24 :6420–6424.

Buscio V , Jiménez MG, Vilaseca M,Grimau VL, Crespi M , Bouzán,CG. Reuse of Textile Dyeing Effluents Treated with Coupled Nanofiltration and Electrochemical Processes. Materials 2016; 9, 490.

Calvete T, Lima EC, Cardoso NF, Dias,SLP, Pavan FA. Application of carbon adsorbents prepared from the Brazilian pine-fruit-shell for the removal of Procion Red MX 3B from aqueous solution—Kinetic, equilibrium, and thermodynamic studies. Chemical Engineering Journal 2009;155: 627–636.

Carneiro JO, Samantilleke AP, Parpot P, Fernandes F, Pastor M, Correia A, Luís EA, Chivanga Barros AA, Teixeira V. Visible Light Induced Enhanced Photocatalytic Degradation of Industrial Effluents (Rhodamine B) in Aqueous Media Using TiO2 Nanoparticles. Journal of Nanomaterials 2016 .

Castañeda - Díaz J, Pavón – Silva T , Gutiérrez - Segura E , Colín – Cruz,A. Electrocoagulation-Adsorption to Remove Anionic and Cationic Dyes from Aqueous Solution by PV-Energy. Journal of Chemistry 2017.

Corda NC, Srinivas Kini. A Review on Adsorption of Cationic Dyes using Activated Carbon. MATEC Web of Conferences 2018.

Demirbas O, Turan Y, Alkan M. Thermodynamics

and kinetics of adsorption of a cationic dye onto sepiolite. Desalination and water treatment 2014;54(3): 1-8.

Deng Y, Zhao R. Advanced Oxidation Processes (AOPs) in Wastewater Treatment. Current Pollution Reports 2015;1:167–176.

Di Biase E, Sarkisov L. Molecular simulation of multi-component adsorption processes related to carbon capture in a high surface area, disordered activated carbon. Carbon 2015 ;94:27–40.

Doczekalska B, Kuśmierek K, ŚwiątkowskiA, & Bartkowiak M. Adsorption of 2,4-dichlorophenoxyacetic acid and 4-chloro-2-metylphenoxyacetic acid onto activated carbons derived from various lignocellulosic materials. Environnemental Science and Heath, part B 2018.

Dos Santos DC, Adebayo MA, Lima EC, Pereira, S F P,Cataluna R, Saucier C, Thue PS, Machado MF.Application of Carbon Composite Adsorbents Prepared from Coffee Waste and Clay for the Removal of Reactive Dyes from Aqueous Solutions Journal of the Brazilian Chemical Society 2015; 26: 924-938.

El Haddad M, Slimani R, Mamouni R, El Antri S , Lazar S. Removal of two textile dyes from aqueous solution onto calcined bones. the Association of Arab Universities for Basic and Applied Sciences onto calcined bones 2013;14: 51 –59.

El-Sayed GO, Yehia MM, Asaad AA. Assessment of activated carbon prepared from corncob by chemical activation with phosphoric acid. Water Resources and Industry 2014 ;7-8:66–75.

Erdem B, Erdem M, ozcan,A S.Adsorption of Reactive Black 5 onto quaternized 2-dimethylaminoethyl methacrylate based polymer / clay Nanocomposites. Adsorption 2016;22(4-6): 767–776.

Fil BA,Yilmaz MT, Bayar S,Elkoca MT. Investigation of adsorption of the dye stuff astrazon red violet 3RN (Basic Violet16) on montmorillonite. Brazilian Journal of Chemical Engineering 2015;31: 171 – 182.

Foo KY, Hameed, BH. Insights into the modeling of adsorption isotherm systems. Chemical Engineering Journal 2010;156: 2–10.

Freundlich HMF. Uber die adsorption in losungen, Zeitschrift fur Physikalische Chemie 1906; 57, 385-470.

Gautam RV, Gautam PK, Banerjee S,Rawat V, Soni S, Sharma SK, Chattopadhyaya MC. Removal of tartrazine by activated carbon biosorbents of Lantana camara: Kinetics, equilibrium modeling and spectroscopic analysis. Environmental Chemical Engineering 2015 ;3 :79–88

Ghaedi AM,Baneshi MM, Vafaei A, Nejad ARS, Tyagi I, Kumar N, Galunin E, Tkachev AG, Agarwal S, Gupta VK. Comparison of multiple linear regression and group method of data handling models for predicting sunset yellow dye removal onto activated carbon from oak tree wood. Environmental Technology & Innovation 2018.

Ghaedi M, Hossainian H, Montazerozohori M,Shokrollahi A, Shojaipour F,Soylak M, Purkait MK. A novel acorn based adsorbent for the removal of brilliant green. Desalination 2011 ;281: 226–233.

Gopinathan R, Bhowal A, Garlapati C. Thermodynamic study of some basic dyes adsorption from aqueous solutions on activated carbon and new correlations. Journal of Chemical. Thermodynamics 2016.

Gurdeep R. Surface Chemistry. Krishna Prakashan Media .2002.

Heibati B, Rodriguez-Couto S, Turan NG ,Ozgonenel O,Albadarin AB,Asif A, Tyagi I   Agarwal S, Gupta VK. Removal of noxious dye—Acid Orange 7 from aqueous solution using natural pumice and Fe-coated pumice stone. Journal of Industrial and Engineering Chemistry 2015;31: 124–131.

HO YS, Mckay G. Pseudo-second order model for sorption processes, Process Biochemistry 1999; 34:451-465

Inyinbor AA, Adekola FA.,Olatunji GAJ.Kinetics, isotherms and thermodynamic modeling of liquid phase adsorption of Rhodamine B dye onto Raphiahookerie fruit epicarp.Water Resources and Industry 2016;15:14–27.

Jain R, Sikarwar S. Adsorptive Removal of Erythrsoine dye onto activated low cost de-oiled mustard. Journal of Hazardous Materials 2009;164:627-633

Jayaraman K. Adsorption and Wetting in Model Mesoporous Silicas and in Complex Metal Oxide Catalysts. Spring, South Orange, New Jersey.2017.

Karimi R, Yousefi F,Ghaedi M, Dashtian K, Montazerozohori M. Efficient adsorption of erythrosine and sunset yellow onto modified palladium nanoparticles with a 2-diamine compound: Application of multivariate technique. Industrial and Engineering Chemistry 2016 ;48 : 43–55.

Karimifard S,Moghaddam MRA. Application of response surface methodology in physicochemical removal of dyes from wastewater: A critical review. Science of the Total Environment 2018 ; 640 –641 : 772 –797.

Kumar R, Ansari MO, Barakat MA. Adsorption of Brilliant Green by Surfactant Doped Polyaniline/ MWCNTs Composite: Evaluation of the Kinetic, Thermodynamic, and Isotherm. Industrial & Engineering Chemistry Research 2014; 53: 7167 –7175.

Kusmierek K, Swiatkowski A. The influence of different agitation techniques on the adsorption kinetics of 4-chlorophenol on granular activated carbon. Reaction Kinetics, Mechanisms and Catalysis 2015 ; 116:261–271.

Lagergen S. Zu theorie der sogenantnen adsorption geloster stoffe, Kungliga Svenska vetenskapsakademiens. Handlingar 1898; 24: 1–39.

Largitte L, Pasquier R. A review of the kinetics adsorption models and their application to the adsorption of lead by an activated carbon. Chemical Engineering Research and Design 2016.

Li F, Xia Q, Gao Y, Cheng Q , Ding L, Yang B, Tian Q, Ma C, Sandac w , Liu Y. Anaerobic biodegradation and decolorization of a refractory acid dye by a forward osmosis membrane bioreactor. Environmental Science Water Research & Technology 2018; 2: 272-280.

Li Y, Du Q , Liu T, Sun J , Jiao Y, Xia Y, Xia L, Wang Z, Zhang W, Wang K, Zhu H, Wu D. Equilibrium, kinetic and thermodynamic studies on the adsorption of phenol onto graphene. Materials Research Bulletin 2012 ;47:1898–1904.

LiuY, Xu H,Yang S F, Tay J H. A general model for biosorption of Cd^{2+}, Cu^{+2} and Zn^{+2} by aerobic granules. Journal of Biotechnology 2003 ;102 :233-239

Luo X P, Fu SY, Du YM, Guo JZ, Li B. Adsorption of methylene blue and mala chite green from aqueous solution by sulfonic acid group modified MIL-101. Microporous and Mesoporous

Materials 2017 ;237: 268-274.

Machado MF, Bergmann CP, Fernandes THM, Lima EC, Royer B, Calvete T, Fagan SB. Adsorption of Reactive Red M-2BE dye from water solutions by multi-walled carbon nanotubes and activated carbon. Hazardous Materials 2011; 192: 1122–1131.

Mane VS, Vijay Babu PV. Studies on the adsorption of Brilliant Green dye from aqueous solution onto low-cost NaOH treated sawdust. Desalination 2011; 273: 321 –329.

Manera C, Tonello AP, Perondi D , Godinho M. Adsorption of leather dyes on activated carbon from leather shaving wastes: kinetics, equilibrium and thermodynamics studies. Environmental Technology 2018.

Mclintock IS. The Elovich Equation in Chemisorption Kinetics. Nature 1967;216: 1204-1205.

Mohd AA, Nur AAP, Bello OS. Kinetic, equilibrium and thermodynamic studies of synthetic dye removal using pomegranate peel activated carbon prepared by microwave-induced KOH activation. Water Resources and Industry 2014; 6:18–35.

Mukhlish MZB, Khan MMR, Islam AR , Akanda ANMS. Removal of reactive dye from aqueous solution using coagulation–flocculation coupled with adsorption on papaya leaf. Mechanical Engineering and Sciences 2016;10: 1884-1894.

Özdemir CS, Önal Y. Error Anlaysis Studies of Dye Adsorption onto Activated Carbon From Aqueous Solutions. Particulate Science and Technology: An International Journal 2013.

Prashanthi M, Sundaram R, Jeyaseelan A, Kaliannan T. Bioremediation and Sustainable Technologies for Cleaner Environment .2017.

Regti A, Laamari MR, Stiriba S, El Haddad, MJ. Potential use of activated carbon derived from Persea species under alkaline conditions for removing cationic dye from wastewaters. Journal of the Association of Arab Universities for Basic and Applied Sciences 2017;24: 10–18 .

Rahman SS, Alif FA., Hossain MM.Optimization of conditions for the biological treatment of textile dyes using isolated soil bacteria. F1000 Research .2018; 7:351.

Rehman R, Mahmud T, Irum M. Brilliant Green Dye Elimination from Water using Psidium guajava Leaves and Solanum tuberosum Peels as Adsorbents in Environmentally Benign Way, Journal of Chemistry 2015.

Roosta M ,Ghaedi M, Daneshfar A, Darafarin S, Sahraei R, Purkait M K . Simultaneous ultrasound-assisted removal of sunset yellow and erythrosine by ZnS:Ni nanoparticles loaded on activated carbon: Optimization by central composite design. Ultrasonics Sonochemistry 2014;21 :1441–1450.

Salem MA, Elsharkawy RG, Hablas MF. Adsorption of Brilliant Green dye by polyaniline/silver nanocomposite: Kinetic, equilibrium, and thermodynamic studies 2015.

Saputra OA, Rachma A H, Handayani DS. Adsorption of Remazol Brilliant Blue R Using Amino-Functionalized Organosilane in Aqueous Solution. Indonesian Journal of Chemistry 2017 ;3 : 343 – 350.

Srenscek -Nazzal JS, Narkiewicz U, Morawski AW,. Wrobel RJ , Michalkiewicz B. Comparison of Optimized Isotherm Models and Error Functions for Carbon Dioxide Adsorption on Activated Carbon. Chemical & Engineering Data 2015;60:3148 –3158.

Takdastan A,Mahvi A H, Lima EC, Shirmardi M, kbarBabaei AA, Goudarzi G, Neisi A, Farsani MH,Vosoughi.Preparation, characterization, and application of activated carbon from low-cost material for the adsorption of tetracycline antibiotic from aqueous solutions ,Journal of Water Science Technology.2016

Treybal RE.Mass Transfer Operations.2nd Edition, McGraw Hill, NewYork.1968.

Thommes M, Kaneko K, Neimark A V, Olivier JP, Rodriguez-Reinoso F, Rouquerol J, Sing K S W. Physisorption of gases, with special reference to the evaluation of surface area and pore size distribution (IUPAC Technical Report). Pure and Applied Chemistry.2015; 87:1051–1069 .

Tunali S, Ozcan AS, Ozcan A, Gedikbey T. Kinetics and equilibrium studies for the adsorption of Acid Red 57 from aqueous solutions onto calcined-alunite. Journal of Hazardous. Materials. 2016;B135 :141–148.

Uday USP, Mahata N, Sasmal S, Bandyopadhyay TK, Mondal A, Bhunia B. .Environmental pollutants and their bioremediation approaches. Dyes contamination in environments, their ecotox-

icological effects, health hazards, and biodegra-
dation and bioremediation mechanisms for en-
vironmental cleanup. Environmental Pollutants
and their Bioremediation Approaches, Ram
Naresh Bharagava, CRC Press; 2017; P.127-176

Uruj T, Azra Y, Umair HKJ. Phytoremediation: Po-
tential flora for synthetic dyestuff metabolism.
Journal of .King Saud University Science. 2016;
28: 119-130.

Vargas AMM, Cazetta AL, Kunita MK, Silva
TL,Almeida VC.Adsorption of methylene blue
on activated carbon produced from flamboy-
ant pods (Delonixregia): Study of adsorption
isotherms and kinetic models . Chemical En-
gineering Journal. 2011;168:722–730.

Wawrzkiewicz M, Hubicki Z. Anion Exchange Resins
as Effective Sorbents for Removal of Acid, Reac-
tive, and Direct Dyes from Textile Wastewaters.
Ion Exchange Ayben Kilislioglu, IntechOpen;
2015, p.37-70.

Xu L , Zheng X, Cui H, Zhu Z, Equilibrium, Kinetic
and Thermodynamic studies on the Adsorp-
tion of Cadmium from Aqueous Solution by
Modified Biomass Ash. Bioinorganic Chemis-
try and Applications 2017.

Zazouli M, Azari A, Dehghan S.,Malekkolae R S.
Adsorption of methylene blue from aqueous
solution onto activated carbons developed from
eucalyptus bark and Crataegus oxyacantha
core. Water Science & Technology,2016.

Zhang B, Ma Z, Yang F, Liu Y, Guo M.Adsorption
properties of ion recognition rice straw lig-
nin on PdCl42−:Equilibrium, kinetics and
mechanism, Colloids and Surfaces A: Physi-
cochemical and Engineering Aspects .2017;514
:260–268 .

Abbreviations

A°   Angstrom
CAG Granular activated carbon
C^0 Initial concentration
C_e Residual concentration at equilibrium
C_t residual concentration at time t
Eq   Equation
h^0 Initial sorption rate for pseudo-second-order adsorption
k_1 Pseudo-first-order adsorption rate constant
k_2 Pseudo-second-order adsorption rate constant

K   Binding constant
k_{AV} Avrami kinetic constant
K_F Freundlich isotherm constant
K_g Equilibrium constant of Liu isotherm
K_L Equilibrium constant of Langmuir isotherm
k_N kinetic adsorption rate constant
m   Mass
N   Total number of experimental data
n   Order of adsorption
n_{AV} Avrami fractional adsorption order
n_F Adsorption intensity
n_L Dimensionless exponent of the Liu equation
P   Number of parameters of the fitted model
pH   Potential of hydrogen
Pr   Pression
q_e Adsorbed amount at equilibrum
q_m maximum adsorption capacity
q_t Adsorbed amount at time t
R   universal gas constant
R^2 Coefficient of determination
RSS   Residual sum squares
R^2_{adj} Adjusted R-squared
SD   Standard deviation
SEM   Scanning electron microscope
T   Temperature
t   Time
V   Volume
v   Agitation speed
V_{ads} Adsorbed volume
   Reduced Chi-squared
λ_{max} Wavelength of maximum absorbance
α   Initial adsorption rate
β   Adsorption constant related to the surface coverage
ΔH^0 Adsorption enthalpy
ΔG^0 Free energy of adsorption
ΔS^0 Adsorption entropy